

Accurate determination of the electric dipole matrix elements, lifetimes, polarizabilities and light-shift ratios in Ba⁺ and Ra⁺

B. K. Sahoo ^{*}, R. G. E. Timmermans and K. Jungmann¹

¹*KVI, University of Groningen, NL-9747 AA Groningen, The Netherlands*

(Dated: November 11, 2019)

We have employed the relativistic coupled-cluster theory to calculate the electric dipole matrix elements in the singly ionized barium (Ba⁺) and radium (Ra⁺). Matrix elements of Ba⁺ are used to determine the light-shift ratios for two different wavelengths on which recent experiments are carried out. By combining the measured light-shift ratios and our calculations, we are able to estimate possible errors associate with the used matrix elements in Ba⁺. Static polarizabilities of the low-lying states and lifetimes of the first excited P-states are also determined using these matrix elements in Ba⁺. A similar approach has been followed to estimate the lifetimes and light-shift ratios in Ra⁺.

PACS numbers: 31.15.Ar,31.15.Dv,31.25.Jf,32.10.Dk
Keywords: Ab initio method, polarizability

I. INTRODUCTION

Recently, both the singly ionized barium (Ba⁺) and (Ra⁺) are proposed as suitable candidates for the parity non-conservation (PNC) experiments [1, 2]. These candidates are also suitable for the atomic clock experiments [3, 4, 5]. Accurate determination of the electric dipole (E1) matrix elements are essential in achieving sub-one percent PNC amplitudes in the above candidates [2, 6]. They are also crucial in determining the dipole polarizabilities accurately which are required to estimate shifts due to the stray electric fields applied [5, 7] during the measurements in the above proposed experiments. There is no direct method to measure them experimentally. Mainly, these results are estimated from the branching ratio (lifetime) measurements from various states. However, when branching ratios of two or more different channels from a given state are relatively significant, it is not possible to estimate the E1 matrix elements precisely. There are a few branching ratio [8, 9, 10] and lifetime [11, 12, 13] measurements of the first P-states available in Ba⁺, although they are not very precise to estimate the E1 matrix elements accurately. On the otherhand, such experiments are not available yet in Ra⁺.

It is also possible to calculate the above matrix elements accurately using a highly potential many-body method. Ba⁺ and Ra⁺ are heavy systems implying both the electron correlation and relativistic effects will be much stronger in these systems. Variety of relativistic many-body methods have already been employed to calculate the E1 matrix elements in the considered systems [14, 15, 16, 17, 18]. But the results obtained by all these works differ at significant precision for which they can be used to determine sub-one percent accuracy of the PNC amplitudes or other experimentally measured quantities like light-shift ratios [19, 20] in the considered systems.

In this work, we have employed the relativistic coupled-cluster (RCC) method to account more electron correlation effects through the non-linear terms for the determination of many E1 matrix elements in both Ba⁺ and Ra⁺. These results are then used to evaluate the light-shift ratios in Ba⁺ at two wavelengths on which experiments were conducted [19, 20]. By analyzing the trends of contributions to the light-shift ratios and transition probabilities, we try to give the upper limits to some of the important matrix elements by combining with the experimental result in that system. The matrix elements are further used to determine the lifetimes and static dipole polarizabilities in Ba⁺. By following the same procedure, we determine in Ra⁺ the lifetimes of the first excited P-states and light-shift ratios at the same wavelengths in which experiments were carried out in Ba⁺.

II. THEORY AND METHOD OF CALCULATIONS

The shift of energy in an atomic state $|\gamma, J, M\rangle$, where J represents the total angular momentum of the state with its azimuthal component M and γ is the additional index representing other required quantum numbers, due to non-resonant ac light in an average period of light oscillations and neglecting the mixing of the magnetic sub-levels is given by [21, 22]

$$\Delta\mathcal{E}(\gamma, J, M) = -\frac{\alpha_0}{2}|\vec{\mathbf{E}}|^2 - i\frac{\alpha_1}{2}\frac{M}{J}(i|\vec{\mathbf{E}}^* \times \vec{\mathbf{E}}|) - \frac{\alpha_2}{2}\left(\frac{3M^2 - J(J+1)}{J(2J-1)}\right)\frac{3E_z^2 - |\vec{\mathbf{E}}|^2}{2} \quad (2.1)$$

where $\vec{\mathbf{E}}$ is the applied vector electric field and E_z is its magnitude in the z-component. Here α_0 , α_1 and α_2 are the scalar, vector and tensor polarizabilities of the state $|\gamma, J, M\rangle$. This expression differs by the term containing vector polarizability when the dc electric field is applied.

^{*}B.K.Sahoo@rug.nl

Using the first-order time-dependent perturbation theory and assuming large detuning from resonance with the applied electric field, the scalar, vector and tensor dynamic polarizabilities of $|\gamma, J, M\rangle$ given as [21, 23]

$$\alpha_0(\gamma, J, M) = -\frac{2}{3[J]} \sum_{K \neq J} \frac{E_J - E_K}{(E_J - E_K)^2 - \omega^2} |\langle \gamma' K || D || \gamma J \rangle|^2 \phi_0(J, K) \quad (2.2)$$

$$\alpha_1(\gamma, J, M) = -\frac{1}{[J]} \sum_{K \neq J} \frac{\omega}{(E_J - E_K)^2 - \omega^2} |\langle \gamma' K || D || \gamma J \rangle|^2 \phi_1(J, K) \quad (2.3)$$

$$\alpha_2(\gamma, J, M) = -\frac{2}{3[J]} \sum_{K \neq J} \frac{E_J - E_K}{(E_J - E_K)^2 - \omega^2} |\langle \gamma' K || D || \gamma J \rangle|^2 \phi_2(J, K), \quad (2.4)$$

respectively, where D is the E1 operator, $[J]$ is the degeneracy factor equal to $2J + 1$, γ' and K represent different states than $|\gamma, J, M\rangle$ with opposite parity, matrix elements with double bars represent the reduced matrixes, $E_{J/K}$ represent energies of the corresponding states in the absence of the external electric field and ω is the frequency of the applied electric field.

The scalar factors $\phi_i(J, K)$'s ($i = 0, 1, 2$) multiplied in the above equations are defined as

$$\phi_0(J, K) = \delta_{J-1, K} + \delta_{J, K} + \delta_{J+1, K} \quad (2.5)$$

$$\phi_1(J, K) = -\frac{1}{J} \delta_{J-1, K} - \frac{1}{J(J+1)} \delta_{J, K} + \frac{1}{J+1} \delta_{J+1, K} \quad (2.6)$$

$$\phi_2(J, K) = -\delta_{J-1, K} + \frac{2J-1}{J+1} \delta_{J, K} - \frac{J(2J-1)}{(J+1)(2J+3)} \delta_{J+1, K}. \quad (2.7)$$

The static dipole polarizabilities can be determined by substituting ω as zero in the above equations.

In fact, the vector shift is maximal than other two shifts for the purely circular polarized light when it is aligned with any existing magnetic field [24, 25]. In this case, it is possible to measure the ratio of light shifts instead of measuring the light shifts or light intensities directly. Mathematically, it is equivalent to say as the following; the ratio of the shift in energies of two different states ($|\gamma_i, J_i, M_i\rangle$ and $|\gamma_f, J_f, M_f\rangle$) is given by

$$R = \frac{\Delta \mathcal{E}(\gamma_i, J_i, M_i)}{\Delta \mathcal{E}(\gamma_f, J_f, M_f)} = \frac{\alpha_1(\gamma_i, J_i, M_i)}{\alpha_1(\gamma_f, J_f, M_f)}, \quad (2.8)$$

which is known as the light-shift ratio in the literature [19, 20].

The probability coefficient (in s^{-1}) due to the allowed

transition is given by

$$A_{f \rightarrow i}^{\text{E1}} = \frac{2.02613 \times 10^{18}}{\lambda^3 [J_f]} S_{f \rightarrow i}^{\text{E1}}, \quad (2.9)$$

where λ (\AA) and $S_{f \rightarrow i}^{\text{E1}} (= |\langle f || D || i \rangle|^2)$ (au) are the wavelengths and strengths of the corresponding transitions, respectively.

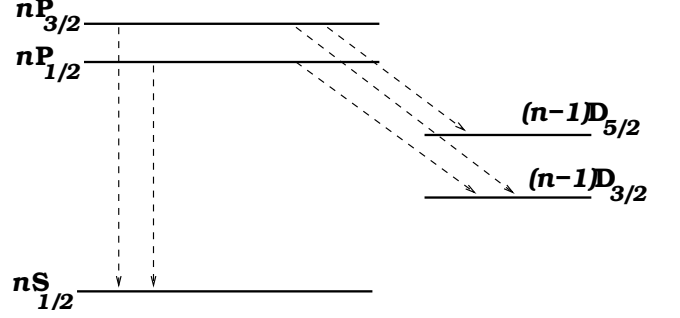


FIG. 1: Schematic low-lying energy level diagrams and decay of the P-states in Ba⁺ and Ra⁺. $n = 6$ and $n = 7$ in Ba⁺ and Ra⁺, respectively.

As seen in Fig. 1, the first excited P-states in both Ba⁺ and Ra⁺ can decay either to the ground S-states directly or via the excited D-states through the allowed transitions. The lifetimes of these P-states can be evaluated from the inverse of the corresponding net transition probabilities due to all possible transition channels. Therefore, the net transition probabilities for the P-states are given by

$$A_{nP_{1/2}} = A_{nP_{1/2} \rightarrow nS_{1/2}} + A_{nP_{1/2} \rightarrow (n-1)D_{3/2}} \quad (2.10)$$

$$A_{nP_{3/2}} = A_{nP_{3/2} \rightarrow nS_{1/2}} + A_{nP_{3/2} \rightarrow (n-1)D_{3/2}} + A_{nP_{3/2} \rightarrow (n-1)D_{5/2}} \quad (2.11)$$

and hence, the lifetimes (in s) of these states are given by

$$\tau_{nP_{1/2}} = \frac{1}{A_{nP_{1/2}}} \quad (2.12)$$

$$\tau_{nP_{3/2}} = \frac{1}{A_{nP_{3/2}}}, \quad (2.13)$$

where $n = 6$ and $n = 7$ in Ba⁺ and Ra⁺, respectively.

Since the transition wavelengths can be determined from the excitation energies from the corresponding transitions, it is clear from the above equations that both the polarizabilities and transition probabilities depend upon the excitation energies (or wavelengths) and E1 matrix elements. Since our motivation in the present work is to verify the accuracies of the E1 matrix elements, we consider the experimental (observational) excitation energies (wavelengths) for our purpose and analyze only the role of the E1 matrix elements from our calculations.

We employ the RCC theory for the Dirac-Coulomb Hamiltonian in the single and double excitations approximation along with the important triple excitations

(CCSD(T) method) to calculate the atomic wave functions in both Ba^+ and Ra^+ . In this procedure, we express the one valence (v) configuration state function as [26, 27]

$$|\Psi_v\rangle = e^T \{1 + S_v\} |\Phi_v\rangle, \quad (2.14)$$

where the reference state $|\Phi_v\rangle$ is constructed by appending the corresponding valence orbital to the closed-shell Dirac-Fock (DF) wave function $|\Phi_0\rangle$; which in second quantization formalism is expressed as $|\Phi_v\rangle = a_v^\dagger |\Phi_0\rangle$. In the above equation, T and S_v are the core and valence-core correlation operators. In the linear approximation,

the above equation yields the form

$$|\Psi_v\rangle = \{1 + T + S_v\} |\Phi_v\rangle. \quad (2.15)$$

As shown in the earlier works, contributions (electron correlation effects) from higher triple and quadrupole excitations arise through the non-linear terms in the CCSD(T) method and their contributions to the various properties in the heavy systems are significantly large [28, 29].

The reduced transition matrix elements $\langle \Psi_f || D || \Psi_i \rangle$ between two states $|\Psi_f\rangle$ and $|\Psi_i\rangle$ are evaluated by

$$\langle \Psi_f || D || \Psi_i \rangle = \frac{\langle \Phi_f || \{1 + S_f^\dagger\} \bar{D} \{1 + S_i\} || \Phi_i \rangle}{\sqrt{\langle \Phi_f || \{1 + S_f^\dagger\} \bar{N} \{1 + S_f\} || \Phi_f \rangle \langle \Phi_i || \{1 + S_i^\dagger\} \bar{N} \{1 + S_i\} || \Phi_i \rangle}} \quad (2.16)$$

where $\bar{D} = e^{T^\dagger} D e^T$ and $\bar{N} = e^{T^\dagger} e^T$ are the non-truncative series in the ordinary RCC theory. However, in the CCSD(T) method, only up to the effective three-body terms, when they are expanded using the general Wick's theorem, of these series will contribute to the above expression. These terms are calculated step by

step and sandwiched between the necessary S_v operators to evaluate the matrix elements. In order to estimate the errors associate with the calculated E1 matrix elements, we check the convergence of these results using both the length and velocity gauge expressions which at the single orbital level are given by

$$\langle f || d || i \rangle = \langle \kappa_f || C^{(1)} || \kappa_i \rangle \int_0^\infty dr \left\{ r [P_f(r) P_i(r) + Q_f(r) Q_i(r)] - \frac{\alpha}{5} (\epsilon_i - \epsilon_f) \left(\frac{\kappa_i - \kappa_f}{2} [P_f(r) Q_i(r) + Q_f(r) P_i(r)] + [P_f(r) Q_i(r) - Q_f(r) P_i(r)] \right) \right\}$$

in the length form and

$$\langle f || d || i \rangle = \langle \kappa_f || C^{(1)} || \kappa_i \rangle \frac{1}{\alpha(\epsilon_i - \epsilon_f)} \int_0^\infty dr \{ (\kappa_i - \kappa_f) [P_f(r) Q_i(r) + Q_f(r) P_i(r)] - [P_f(r) Q_i(r) - Q_f(r) P_i(r)] \} \quad (2.18)$$

in the velocity form, respectively. In these expressions, $C^{(1)}$ is the Racah vector with rank one, $P_{i/f}(r)$ and $Q_{i/f}(r)$ are the large and small components of the Dirac single particle orbitals, $\kappa_{i/f}$ are the relativistic quantum numbers, $\epsilon_{i/f}$ are the single particle energies and α is the fine structure constant.

III. RESULTS AND DISCUSSIONS

A. Ba^+

We present our calculated E1 matrix elements of Ba^+ in Table I. The reported error bars in these results except from the matrix elements related to the D- and F- states are estimated from the differences between the length and velocity gauge results. It was rather difficult to converge

the velocity gauge results for the D- and F- states, therefore we consider the difference between the converged length gauge results using the CCSD(T) method and just by single and double excitations approximation (CCSD method), which are assumed as the upper limit to the contributions due to the neglected excitations, as the error bars. However, these error bars are just used to estimate errors in the light-shift ratio calculations in the considered system and we analyze the accuracy of these results later by fitting with the experimentally measured values of the light-shift ratios at two different wavelengths as discussed below.

We also compare our results with the earlier works in Table I. As seen, most of the important low-lying E1 matrix elements from various works differ at the second decimal places which means the difference is mainly due to the different many-body methods employed and they

TABLE I: Absolute magnitudes of the reduced dipole matrix elements in Ba^+ . Estimated error bars from this work given inside the parenthesis.

Transition	Present	Ref. [14]	Ref. [15]	Ref. [16]	Ref. [17]
$6p_{1/2} \rightarrow 6s_{1/2}$	3.36(1)	3.310	3.3266	3.3357	3.300
$7p_{1/2} \rightarrow 6s_{1/2}$	0.10(1)	0.099	0.1193	0.0621	
$8p_{1/2} \rightarrow 6s_{1/2}$	0.11(5)	0.115	0.4696		
$6p_{3/2} \rightarrow 6s_{1/2}$	4.73(3)	4.674	4.6982	4.7065	4.658
$7p_{3/2} \rightarrow 6s_{1/2}$	0.17(5)	0.035	0.3610	0.0868	
$8p_{3/2} \rightarrow 6s_{1/2}$	0.11(5)	0.073	0.5710		
$6p_{1/2} \rightarrow 7s_{1/2}$	2.44(4)	2.493	2.3220		
$6p_{1/2} \rightarrow 8s_{1/2}$	0.66(5)	0.705	0.7283		
$6p_{3/2} \rightarrow 7s_{1/2}$	3.80(2)	3.882	3.6482		
$6p_{3/2} \rightarrow 8s_{1/2}$	0.97(5)	1.025	1.0518		
$6p_{1/2} \rightarrow 5d_{3/2}$	3.11(3)	3.055	2.9449		3.009
$7p_{1/2} \rightarrow 5d_{3/2}$	0.28(2)	0.261	0.3050		
$8p_{1/2} \rightarrow 5d_{3/2}$	0.13(2)	0.119	0.1121		
$6p_{3/2} \rightarrow 5d_{3/2}$	1.34(2)	1.334	1.2836		1.312
$7p_{3/2} \rightarrow 5d_{3/2}$	0.16(1)	1.472	0.1645		
$8p_{3/2} \rightarrow 5d_{3/2}$	0.07(2)	0.070	0.0650		
$4f_{5/2} \rightarrow 5d_{3/2}$	3.75(11)				
$5f_{5/2} \rightarrow 5d_{3/2}$	1.59(8)				
$6f_{5/2} \rightarrow 5d_{3/2}$	0.17(2)				
$6p_{3/2} \rightarrow 5d_{5/2}$	4.02(7)	4.118	3.9876		4.057
$7p_{3/2} \rightarrow 5d_{5/2}$	0.46(1)	0.432	0.4788		
$8p_{3/2} \rightarrow 5d_{5/2}$	0.21(2)	0.206	0.1926		
$4f_{5/2} \rightarrow 5d_{5/2}$	1.08(4)				
$5f_{5/2} \rightarrow 5d_{5/2}$	0.45(7)				
$6f_{5/2} \rightarrow 5d_{5/2}$	0.15(2)				
$4f_{7/2} \rightarrow 5d_{5/2}$	4.84(5)				
$5f_{7/2} \rightarrow 5d_{5/2}$	2.47(6)				
$6f_{7/2} \rightarrow 5d_{5/2}$	1.04(7)				
$6p_{1/2} \rightarrow 6d_{3/2}$	4.89(10)				
$6p_{1/2} \rightarrow 7d_{3/2}$	1.50(8)				
$6p_{3/2} \rightarrow 6d_{3/2}$	2.33(7)				
$6p_{3/2} \rightarrow 7d_{3/2}$	0.67(4)				
$6p_{3/2} \rightarrow 6d_{5/2}$	6.91(21)				
$6p_{3/2} \rightarrow 7d_{5/2}$	2.01(5)				

may not be due to the numerical methods used in the calculations. That is the reason why we have presented our results up to the second decimal places in the above table. As a matter of fact, correct results up to the second decimal places are crucial in obtaining the light-shift ratios correctly as will be shown below. First, we would like to briefly discuss here the important differences in the various works presented in Table I. Geetha et al. [15] have employed the same approach like ours, but they had used part numerical orbitals using GRASP and part analytical orbitals using Gaussian type orbitals (GTOs). In the present work, we have considered pure analytical orbitals using GTOs. Another difference between these two works is that \bar{D} of Eq. (2.16) is truncated only at the effective one-body terms by Geetha et al. [30], where other higher order terms have been considered in the

present calculation. The main difference in the methods applied by Dzuba et al. [14] and ours have been discussed by Geetha et al. in their work [15]. In summary, they have employed the Green's function technique which is also an all order perturbative method like ours. In their work, the orbitals are also obtained analytically like the present work. However, the level of approximation in both the works could be different which cannot be obviously distinguished. Iskrenova-Tchoukova and Safronova [16] have used linearized CCSD method with important triple excitations and orbitals have been constructed using the B-spline basis. As has been pointed out earlier, the non-linear terms can incorporate higher order correlation effects which are necessary [28, 29] to account in the considered heavy system. Again, the procedure to consider partial triple excitations in their method and in the present work is different. We consider effects of partial triple excitations by estimating each time their contributions to the energy of the corresponding valence state and then solve the CCSD method amplitudes self-consistently which involves the above energy. However, Iskrenova-Tchoukova and Safronova include them directly in the amplitude determining equations. Guet and Johnson have just applied the relativistic many-body method at the second order approximation (MBPT(2) method) using the B-spline basis to calculate their results in contrast to our method which is all order in nature [27, 28].

We have used our calculated reduced E1 matrix elements and experimental energies [31] in Eq. (2.3) to obtain the dynamic vector dipole polarizabilities (α_1) of the $6S_{1/2}$ and $5D_{3/2}$ states in Ba^+ at two different wavelengths (of external electric fields) and they are presented in Table II. Only $6P_{1/2}$, $7P_{1/2}$, $8P_{1/2}$, $6P_{3/2}$, $7P_{3/2}$, $8P_{3/2}$, $4F_{5/2}$, $5F_{5/2}$ and $6F_{5/2}$ intermediate states (K) have been taken into account as they seem to be the most important contributing states as seen from this table. It can be noticed that the magnitude of α_1 s of the $6S_{1/2}$ state are larger than the $5D_{3/2}$ state at both the wavelengths, but their differences are smaller when the frequency of the external field is small. Again, the sign of these quantities are different at the smaller wavelength (514.53 nm), whereas they are opposite at the large wavelength (1111.68 nm). For both the states, the largest contribution comes from the $6P_{1/2}$ state. The next highest contribution arises from the $6P_{3/2}$ state. The third largest contributions to α_1 of the $5D_{3/2}$ state comes from the $4F_{5/2}$ state. Surprisingly, the rest of the contributions are dominated by the higher F-states compared to the P-states. We have given contributions from pure core correlations, core-valence correlations and higher states those are neglected as "Others". The core correlation effects are around 0.319 au and 0.147 au at the wavelengths 514.53 nm and 1111.68 nm, respectively. These contributions are evaluated using the MBPT(2) method. The possible errors due to the omission of the higher states may come from the neglected F-states which seems to be important in the determination of α_1 of the $5D_{3/2}$ state. Therefore, an approach similar to the one applied

to determine the dynamic scalar and tensor polarizabilities [32] will be more appropriate to use for the high precision light-shift ratio studies in the present system.

Now considering the above results of α_1 for both the $6S_{1/2}$ and $5D_{3/2}$ states and using Eq. (2.8), we obtain the light-shift ratios in Ba^+ as $R^{\lambda=514.53nm} = -11.36(20)$ and $R^{\lambda=1111.68nm} = 0.418(3)$, where core correlations contribute around 0.6% and 1% at the wavelengths 514.53 nm and 1111.68 nm, respectively. The corresponding experimental results are $R^{\lambda=514.53nm} = -11.494(13)$ and $R^{\lambda=1111.68nm} = 0.4176(8)$ at the wavelengths 514.53 nm and 1111.68 nm, respectively [19, 20]. Our results match well with the corresponding experimental results. It shows that accounting core correlation effects are essential for the high precision results in the light-shift studies, although their magnitudes seem to be very small in comparison to the α_1 of the $6S_{1/2}$ state. Especially, their contributions are relatively larger at the higher wavelength (smaller frequency). The errors quoted in our light-shift ratio calculations are obtained from the error bars given for the E1 matrix elements in Table I.

We are now in a position to analyze the accuracy of the E1 matrix elements by studying their contributions to the light-shift ratio calculations. Since contributions from the $6P_{1/2}$ state seems larger, we first analyze matrix elements involving this state. From Table I, we can find that different theoretical predictions of the magnitude (sign is irrelevant for our observable) $\langle 6p_{1/2}||D||6s \rangle$ range from 3.30 au to 3.37 au (along with the error bar). Now keeping all other matrix elements unchanged from our calculations, we observe that light-shift ratios vary from $R^{\lambda=514.53nm} = -10.77$ and $R^{\lambda=1111.68nm} = 0.337$ to $R^{\lambda=514.53nm} = -11.45$ and $R^{\lambda=1111.68nm} = 0.432$. With $\langle 6p_{1/2}||D||6s \rangle = 3.33$, which is reported by Geetha et al. [15] and Iskrenova-Tchoukova and Safronova [16], we observe $R^{\lambda=514.53nm} = -11.06$ and $R^{\lambda=1111.68nm} = 0.337$. Keeping the value of the above matrix element constant, we consider now the range of $\langle 6p_{3/2}||D||6s \rangle$ as 4.66 au to 4.76 au and observe from $R^{\lambda=514.53nm} = -11.21$ and $R^{\lambda=1111.68nm} = 0.432$ to $R^{\lambda=514.53nm} = -10.99$ and $R^{\lambda=1111.68nm} = 0.353$. To improve these results, we fix now $\langle 6p_{3/2}||D||6s \rangle = 4.70$ and vary $\langle 6p_{1/2}||D||6s \rangle$ result again. We find that when we consider $\langle 6p_{1/2}||D||6s \rangle = 3.35$ and $\langle 6p_{1/2}||D||6s \rangle = 3.37$ for $\langle 6p_{3/2}||D||6s \rangle = 4.70$, we get $R^{\lambda=514.53nm} = -11.32$ and $R^{\lambda=1111.68nm} = 0.428$ and $R^{\lambda=514.53nm} = -11.51$ and $R^{\lambda=1111.68nm} = 0.455$, respectively. Since the former result, is little close with the experimental results for both the wavelengths, we now keep $\langle 6p_{1/2}||D||6s \rangle = 3.35$ and increase $\langle 6p_{3/2}||D||6s \rangle$ result and get $R^{\lambda=514.53nm} = -11.27$ and $R^{\lambda=1111.68nm} = 0.412$ and $R^{\lambda=514.53nm} = -11.22$ and $R^{\lambda=1111.68nm} = 0.396$ for 4.72 au and 4.74 au, respectively. Therefore, we conclude now that $\langle 6p_{3/2}||D||6s \rangle$ will be around 4.73 au. Now keeping $\langle 6p_{1/2}||D||6s \rangle = 3.35$ and $\langle 6p_{3/2}||D||6s \rangle = 4.73$ when we vary $\langle 6p_{1/2}||D||5d_{3/2} \rangle$ from 3.00 au to 3.15 au, we

get from $R^{\lambda=514.53nm} = -11.93$ and $R^{\lambda=1111.68nm} = 0.435$ to $R^{\lambda=514.53nm} = -11.02$ and $R^{\lambda=1111.68nm} = 0.394$. Results close to the experimental measurements are able to produce only when $\langle 6p_{1/2}||D||5d_{3/2} \rangle$ is around 3.08 au. Now we keep $\langle 6p_{1/2}||D||6s \rangle = 3.35$, $\langle 6p_{3/2}||D||6s \rangle = 4.73$ and $\langle 6p_{1/2}||D||5d_{3/2} \rangle = 3.08$ then vary $\langle 6p_{3/2}||D||5d_{3/2} \rangle$ matrix element from 1.28 au to 1.36 au. We get light-shift ratios close to experimental results when $\langle 6p_{3/2}||D||5d_{3/2} \rangle$ is around 1.32 au. However, light-shift results vary slowly in the given range of this matrix element while the previous matrix elements considered earlier play the crucial roles in deciding the final results. We now vary $\langle 4f_{5/2}||D||5d_{3/2} \rangle$ matrix element from 3.50 au to 4.00 au by considering $\langle 6p_{1/2}||D||6s \rangle = 3.35$, $\langle 6p_{3/2}||D||6s \rangle = 4.73$, $\langle 6p_{1/2}||D||5d_{3/2} \rangle = 3.08$ and $\langle 6p_{3/2}||D||5d_{3/2} \rangle = 1.32$, we get from $R^{\lambda=514.53nm} = -11.57$ and $R^{\lambda=1111.68nm} = 0.409$ to $R^{\lambda=514.53nm} = -11.36$ and $R^{\lambda=1111.68nm} = 0.418$. By fixing $\langle 4f_{5/2}||D||5d_{3/2} \rangle = 4.00$, when we reshuffle other matrix elements, we get light-shift ratios close to the experimental values for $\langle 6p_{1/2}||D||6s \rangle = 3.35$, $\langle 6p_{3/2}||D||6s \rangle = 4.72$, $\langle 6p_{1/2}||D||5d_{3/2} \rangle = 3.08$ and $\langle 6p_{3/2}||D||5d_{3/2} \rangle = 1.34$. When we keep these matrix elements constant and vary the matrix element of $\langle 4f_{5/2}||D||5d_{3/2} \rangle$, we get the best light-shift ratios for 3.65 au and they correspond to $R^{\lambda=514.53nm} = -11.49$ and $R^{\lambda=1111.68nm} = 0.419$. For any other combinations, the light-shift ratios vary by large amount from the experimental results; at least for one of the wavelengths.

Again, there are also measurements of the transition probabilities in Ba^+ available from three different experiments [8, 9, 10]. We evaluate them using the experimental wavelengths (determined from the corresponding experimental excitation energies [31]) and E1 matrix elements presented in Table I. These results are given in Table III. We have also presented both the experimental and other theoretical results in the same table. It can be clearly noticed that our results in all the cases match well with the experimental results with smaller error bars where as some of the earlier works differ significantly. Differences between all the theoretical works are discussed by Geetha et al. [15].

Now if we consider $\langle 6p_{1/2}||D||6s \rangle$ as 3.35 au as we analyzed from the light-shift ratio studies, we get $A_{6P_{1/2} \rightarrow 6S_{1/2}}$ as $94.566 \times 10^6 s^{-1}$ which is at the marginal lower side error limit of Reader et al experimental result [9]. Our $A_{6P_{1/2} \rightarrow 5D_{3/2}}$ result is also at the marginal upper limit of Kastberg et al experimental result [8]. If we consider $\langle 6p_{1/2}||D||5d_{3/2} \rangle = 3.08$ from the analysis of light-shift ratio studies then we get $A_{6P_{1/2} \rightarrow 5D_{3/2}} = 35.015 \times 10^6 s^{-1}$ which is within the experimental error bar.

By gathering all the informations from the analysis of roles of various matrix elements in the light-shift ratios and transition probabilities studies, we arrive in the conclusion at this point that the magnitude of the following

matrix elements will be

$$\begin{aligned}\langle 6p_{1/2} || D || 6s_{1/2} \rangle &= 3.36(2) \\ \langle 6p_{3/2} || D || 6s_{1/2} \rangle &= 4.73(3) \\ \langle 6p_{1/2} || D || 5d_{3/2} \rangle &= 3.08(3) \\ \langle 6p_{3/2} || D || 5d_{3/2} \rangle &= 1.34(2) \\ \langle 4f_{5/2} || D || 5d_{3/2} \rangle &= 3.73(20).\end{aligned}$$

The above conclusions differ from the findings of the previous work by Sherman et al. [20] who find

$$\begin{aligned}\langle 6p_{1/2} || D || 5d_{3/2} \rangle &= 3.14(3) \\ \langle 4f_{5/2} || D || 5d_{3/2} \rangle &= 4.36(36),\end{aligned}$$

where they had combined with Geetha et al [15] results to estimate these values. Further more, light-shift ratio measurements with a large number of wavelengths are required in order to estimate the above E1 matrix elements more accurately.

There are a number of measurements on the lifetimes of the $6p\ ^2P_{1/2}$ and $6p\ ^2P_{3/2}$ states are available in the literature [11, 12, 13], but the associate error bars of these measurements are very large. We evaluate the net transition probabilities of these states using the above matrix elements and experimental wavelengths [31]. We give these results in Table IV and compare with the corresponding experimental results. Results obtained from other works are also given in the same table. As it can be seen from this table that the lifetime of the $6P_{1/2}$ state is more than 2% difference from the earlier findings which needs to be verified by new experiments. Although, our calculation of the lifetime of the $6P_{3/2}$ state is within the error bar of the experimental results and agree with other findings, but the $A_{6P_{3/2} \rightarrow 5D_{5/2}}$ contributes around 28% in its evaluation. Since the accuracy of the E1 matrix element of $\langle 6p_{3/2} || D || 5d_{5/2} \rangle$ is not verified well as it has been done for the transition matrix elements involved in the determination of lifetime of the $6P_{1/2}$ state, the lifetime of the $6P_{3/2}$ state may be little different than what we find, but it will be within the error bar that we have given (which is large). The error bars given in our lifetime calculations come only from the error bars of the E1 matrix elements as given above.

Since the knowledge of the static dipole polarizabilities of different states in Ba^+ is important to estimate shifts in the energy levels when they are subjected to high precision experiments like atomic clock, PNC and so on, we have calculated these quantities for the first five low-lying states in the given system. Likewise vector polarizabilities, the scalar and tensor static dynamic polarizabilities are evaluated using our E1 matrix elements presented in Table I and their experimental excitation energies [31]. We have considered the $6S_{1/2}$, $7S_{1/2}$, $8S_{1/2}$, $5D_{3/2}$, $6D_{3/2}$, $7D_{3/2}$, $5D_{5/2}$, $6D_{5/2}$, $7D_{5/2}$, $4F_{7/2}$, $5F_{7/2}$ and $6F_{7/2}$ states in these calculations along with the intermediate states considered for the above vector polarizabilities calculations. Again, we have calculated the core correlation effects using the relativistic CCSD

method employed for the closed-shell system in our earlier work [33]. The core-valence and higher state contributions other than the matrix elements reported in Table I are evaluated using the MBPT(2) method. Our static dipole polarizability results of various states in Ba^+ are presented in Table V. The core-correlation effects for the scalar and tensor polarizabilities are 9.582 au and -0.372 au, respectively. There are experimental results available only for the ground state [34, 35]. Again, a couple of theoretical calculations available for the ground state [16, 36, 37, 38]. Except Iskrenova-Tchoukova and Safronova work [16], others have employed molecular codes to determine them. Also, Iskrenova-Tchoukova and Safronova have used the E1 matrix elements from the linearized CCSD(T) method to evaluate the ground state polarizabilities. In their work, they have considered only four important matrix elements to evaluate them and we have considered two more higher excited states matrix elements in this calculation. Again, their core-correlation effects are considered using the lower order many-body methods and it is larger than our finding. There are no other results for the excited states available to compare with our results. The error bars given in our calculations are from the errors given for the E1 matrix elements in Table I. The agreement between our ground state polarizability result with its experimental measurement further supports the accuracy of the E1 matrix elements used in this calculation.

B. Ra^+

We have also followed the same procedure as above to determine the light-shift ratios and lifetimes of the first excited P-states in Ra^+ . We present the various E1 matrix elements used in these calculations in Table VI. The error bars of different matrix elements are estimated using the same procedure followed as in Ba^+ . There are also other calculations available in this system [14, 18]. Dzuba et al. [14] have used the same method as in Ba^+ to calculate these matrix elements. The procedure followed by Safronova et al. [18] is based on the linearized CCSD(T) method like Iskrenova-Tchoukova and Safronova work in Ba^+ [16]. Most of our results match with these calculations, but they still differ at the second decimal places as in Ba^+ .

Since Ra^+ has been proposed for the atomic clock [5] and PNC experiments [2], knowledge of the accuracies of the above E1 matrix elements are essential. We propose also similar light-shift ratio measurements at different wavelengths for the same purpose. As a preliminary study, we consider the same off-resonant wavelengths as have been considered in the Ba^+ experiments [19, 20] and have carried out light-shift ratio calculations. In Table VII, we present the dynamic vector polarizabilities for the $7S_{1/2}$ and $6D_{3/2}$ states at $\lambda = 514.53\text{nm}$ and $\lambda = 1111.68\text{nm}$. We use our E1 matrix elements presented in Table VI with the experimental energies [31]

to evaluate them. In this calculation, we have considered the $7P_{1/2}$, $8P_{1/2}$, $9P_{1/2}$, $7P_{3/2}$, $8P_{3/2}$, $9P_{3/2}$, $5F_{5/2}$, $6F_{5/2}$ and $7F_{5/2}$ intermediate states.

As seen in Table VII, the trend of the contributions from various intermediate states is same as in Ba^+ . The core-correlations are little larger compared to Ba^+ and they are around 0.346 au and 0.159 au at $\lambda = 514.53\text{nm}$ and $\lambda = 1111.68\text{nm}$, respectively. We obtain around $R^{\lambda=514.53\text{nm}} = -6.42(7)$ and $R^{\lambda=1111.68\text{nm}} = 0.017(1)$. The given error bars again come from our estimated accuracies of the E1 matrix elements. Since there are no experimental data available in Ra^+ to check the accuracy of the E1 matrix elements or light-shift ratios, our results will be useful for the future light-shift experiments in this system.

We have already reported polarizabilities of the $7S_{1/2}$, $6D_{3/2}$ and $6D_{5/2}$ states in our earlier work [5]. However, the knowledge of the transition probabilities and lifetimes of the first P-states in the considered states are not known yet. We use our E1 matrix elements reported in Table VI and experimental energies [31] to evaluate them. In Table VIII, we present the transition probabilities of various channels from the $7P_{1/2}$ and $7P_{3/2}$ states. As seen from this table, the relative transition probability of the $7P_{3/2} \rightarrow 7S_{1/2}$ transition is much larger than the $7P_{1/2} \rightarrow 7S_{1/2}$ transition in the present system compared to Ba^+ . Since the wavelength of the $7P_{1/2} \rightarrow 6D_{3/2}$ transition is one order larger here, the corresponding transition probability is comparatively smaller. Hence, the lifetime of the $7P_{1/2}$ state becomes little larger than the $6P_{1/2}$ state in Ba^+ . Again, the lifetime of the $7P_{3/2}$ state becomes smaller than the $6P_{3/2}$ state in Ba^+ due

to the fact that the $7P_{3/2} \rightarrow 7S_{1/2}$ transition probability is much larger. We present the net transition probabilities and lifetimes of the $7P_{1/2}$ and $7P_{3/2}$ states in Table IX. In Ra^+ , $A_{7P_{3/2} \rightarrow 6D_{5/2}}$ contributes only by 12% to the final lifetime determination of the $7P_{3/2}$ state in contrast to 28% in Ba^+ .

IV. CONCLUSION

We have employed the relativistic coupled-cluster theory to calculate the electric dipole matrix elements in the singly ionized barium and radium. These elements are used to determine the light-shift ratios and transition probabilities in the singly ionized barium and comparing with the corresponding experimental data, we have estimated the accuracy of various low-lying matrix elements in this system. Further, we have evaluated the scalar and tensor static dipole polarizabilities and lifetimes in the same system. We have also calculated the light-shift ratios, transition probabilities and lifetimes using our electric dipole matrix elements in the singly ionized radium. These data will be helpful in the future experiments in the considered system.

V. ACKNOWLEDGMENT

This work is supported by NWO under VENI fellowship scheme with project number 680-47-128 and put of the stichting FOM physics program 48 (Tri μ p). We thank Norval Fortson, Jeff Sherman, Bhanu Pratap Das and Dimtry Budker for useful discussions.

-
- [1] N. Fortson, Phys. Rev. Lett. **70**, 2383 (1993).
 - [2] L. W. Wansbeek, B. K. Sahoo, R. G. E. Timmermans, K. Jungmann, B. P. Das and D. Mukherjee, arXiv:0807.1636 (unpublished).
 - [3] J. A. Sherman, W. Trimble, S. Metz, W. Nagourney and N. Fortson, arXiv:physics/0504013.
 - [4] B. K. Sahoo, Phys. Rev. A **74**, 020501(R) (2006).
 - [5] B. K. Sahoo, B. P. Das, R. K. Chaudhuri, D. Mukherjee, R. G. E. Timmermans, and K. Jungmann, Phys. Rev. A **76**, 040504(R) (2007).
 - [6] B. K. Sahoo, R. Chaudhuri, B. P. Das and D. Mukherjee, Phys. Rev. Lett. **96**, 163003 (2006).
 - [7] W. M. Itano, J. Res. Natl. Inst. Stand. Technol. **105**, 829 (2000).
 - [8] A. Kastberg, P. Villemoes, A. Arnesen, F. Hejlskjöld, A. Langereis, P. Jungner and S. Linnaeus, J. Opt. Soc. Am. B **10**, 1330 (1993).
 - [9] J. Reader, C. H. Corliss, W. L. Wiese and G. A. Martin, *Wavelengths and Transitions Probabilities for Atoms and Atomic Ions*, Natl. Bur. Stand. (U.S.) Circ. No. 68, Vol. X, U.S. GPO, Washington, D.C. (1980).
 - [10] A. Gallagher, Phys. Rev. **157**, 24 (1967).
 - [11] P. Kuske, N. Kirchner, W. Wittmann, H. J. Andrä and D. Kaiser, Phys. Lett. **64A**, 377 (1978).
 - [12] E. H. Pinnington, R. W. Berends and M. Lumsden, J. Phys. B **28**, 2095 (1995).
 - [13] H. J. Andrä, *Beam-Foil Spectroscopy*, ed. by I. A. Sellin and D. J. Pegg Plenum, New York, **2**, Pg. 825 (1976).
 - [14] V. A. Dzuba, V. V. Flambaum and J. S. M. Ginges, Phys. Rev. A **63**, 062101 (2001).
 - [15] G. Gopakumar, H. Merlitz, R. K. Chaudhuri, B. P. Das, U. S. Mahapatra and D. Mukherjee, Phys. Rev. **66**, 032505 (2002).
 - [16] E. Iskrenova-Tchoukova and M. S. Safronova, Phys. Rev. A **78**, 012508 (2008).
 - [17] C. Guet and W. R. Johnson, Phys. Rev. A **44**, 1531 (1991).
 - [18] U. I. Safronova, W. R. Johnson and M. S. Safronova, Phys. Rev. A **76**, 042504 (2007).
 - [19] J. A. Sherman, T. W. Koerber, A. Markhotok, W. Nagourney and E. N. Fortson, Phys. Rev. Lett. **94**, 243001 (2005).
 - [20] J. A. Sherman, A. Andalkar, W. Nagourney and E. N. Fortson, arXiv:0808.1826.
 - [21] J. E. Stalnaker, *Progress Towards Parity Nonconservation in Atomic Ytterbium*, Ph.D. thesis, University of California, Berkeley, USA (2005).
 - [22] J. E. Stalnaker, D. Budker, S. J. Freedman, J. S. Guz-

- man, S. M. Rochester and V. V. Yashchuk, Phys. Rev. A **73**, 043416 (2006).
- [23] K. D. Bonin and V. V. Kresin, *Electric-Dipole Polarizabilities of Atoms, Molecules and Clusters*, World Scientific, Chap. 3, Pg. 36 (1997).
- [24] B. S. Mathur, H. Tang and W. Happer, Phys. Rev. **171**, 11 (1968).
- [25] C. Cohen-Tannoudji and J. Dupont-Roc, Phys. Rev. A **5**, 968 (1972).
- [26] D. Mukherjee, R. Moitra and A. Mukhopadhyay, Mol. Physics **33**, 955 (1977).
- [27] I. Lindgren, *A coupled-cluster approach to the many-body perturbation theory for open-shell systems*, In Per-Olov Lwdin and Yngve hrn , editors, Atomic, molecular, and solid-state theory, collision phenomena, and computational methods, International Journal of Quantum Chemistry, Quantum Chemistry Symposium **12**, pages 33-58, John Wiley & Sons, March 1978.
- [28] B. K. Sahoo, S. Majumder, R. K. Chaudhuri, B. P. Das, and D. Mukherjee, J. Phys. B **37**, 3409 (2004).
- [29] B. K. Sahoo, Phys. Rev. A **73**, 062501 (2006).
- [30] B. P. Das, *Private communication*.
- [31] C. E. Moore, Natl. Stand. Ref. Data Ser. (U.S., Natl. Bur. Stand.), **3** (1971).
- [32] L. W. Wansbeek, B. K. Sahoo, R. G. E. Timmermans, B. P. Das and D. Mukherjee, Phys. Rev. A **78**, 012515 (2008).
- [33] B. K. Sahoo and B. P. Das, Phys. Rev. A **77**, 062516 (2008).
- [34] E. L. Snow and S. R. Lundeen, Phys. Rev. A **76**, 052505 (2007)
- [35] T. F. Gallagher, R. Kachru and N. H. Tran, Phys. Rev. A **26**, 2611 (1982).
- [36] I. S. Lim and P. Schwerdtfeger, Phys. Rev. A **70**, 062501 (2004).
- [37] I. Miadokova, V. Kellö and A. J. Sadlej, Theor. Chem. Act. **96**, 166 (1997).
- [38] S. H. patil and K. T. Tang, J. Chem. Phys. **106**, 2298 (1997).

TABLE II: Dynamic vector polarizabilities (in au) at two different wavelengths in Ba⁺.

Intermediate States (K)	$6s_{1/2}$		$5d_{3/2}$	
	$\lambda = 514.53\text{nm}$	$\lambda = 1111.68\text{nm}$	$\lambda = 514.53\text{nm}$	$\lambda = 1111.68\text{nm}$
$6p_{1/2}$	-978.638	-45.080	48.786	-20.419
$7p_{1/2}$	-0.014	-0.006	-0.035	-0.014
$8p_{1/2}$	-0.010	-0.004	-0.004	-0.002
$6p_{3/2}$	305.338	36.717	6.112	-1.121
$7p_{3/2}$	0.019	0.008	-0.004	-0.002
$8p_{3/2}$	0.005	0.002	-5×10^{-4}	-4×10^{-4}
$4f_{5/2}$			3.987	1.541
$5f_{5/2}$			0.153	0.162
$6f_{5/2}$			0.004	0.002
Others	0.301	0.137	0.243	0.177
Total	-672.994(1.944)	-8.223(201)	59.298(1.375)	-19.675(323)

TABLE III: Transition strengths (au), wavelengths (\AA) and probabilities ($\times 10^6 s^{-1}$) from P-states in Ba⁺.

Transition($f \rightarrow i$)	$S_{f \rightarrow i}^{E1}$	$\lambda_{f \rightarrow i}^\dagger$	$A_{f \rightarrow i}^{E1}$	Others	Expt.
$6P_{1/2} \rightarrow 6S_{1/2}$	11.290	4935.5	95.131	93.68 ^a	95(9) ^c
				91.78 ^b	95.5(10) ^d
					95(7) ^e
$A_{6P_{3/2} \rightarrow 6S_{1/2}}$	22.373	4555.3	119.889	119.37 ^a	106(9) ^c
				116.25 ^b	117(4) ^d
					118(8) ^e
$A_{6P_{1/2} \rightarrow 5D_{3/2}}$	9.672	6498.7	35.701	32.609 ^a	33.8(19) ^c
				33.42 ^b	33(8) ^d
					33(4) ^e
$A_{6P_{3/2} \rightarrow 5D_{3/2}}$	1.796	5855.3	4.531	4.255 ^a	4.69(29) ^c
				3.342 ^b	4.8(5) ^d
					4.48(6) ^e
$A_{6P_{3/2} \rightarrow 5D_{5/2}}$	16.160	6143.4	35.305	34.93 ^a	37.7(24) ^c
				35.95 ^b	37(4) ^d
					37(4) ^e

[†] λ s are determined from the experimental excitation energies [31].

References: ^a[15], ^b[17], ^c[8], ^d[9] and ^e[10].

TABLE IV: Net transition probabilities ($\times 10^6 s^{-1}$) and life-times (ns) in Ba^+ .

State(= i)	A_i	τ_i	Others	Expt.
$6P_{1/2}$	130.146	7.68(7)	7.89 ^a 7.92 ^b 7.83 ^c 7.99 ^d	7.92(8) ^e 7.90(10) ^f
$6P_{3/2}$	159.72	6.26(11)	6.30 ^a 6.31 ^b 6.27 ^c 6.39 ^d	6.32(10) ^f 6.312(16) ^g

References: ^a[14], ^b[15], ^c[16], ^d[17], ^e[11], ^f[12] and ^g[13].

TABLE V: Scalar and tensor static ($\omega = 0$) polarizabilities in Ba^+ .

Intermediate States (K)	$6S_{1/2}$	$6P_{1/2}$	$6P_{3/2}$		$5D_{3/2}$		$5D_{5/2}$	
	Scalar	Scalar	Scalar	Tensor	Scalar	Tensor	Scalar	Tensor
$6S_{1/2}$		-40.763	-37.280	37.280				
$7S_{1/2}$		19.714	25.889	-25.889				
$8S_{1/2}$		0.844	0.954	-0.954				
$6P_{1/2}$	40.763				22.992	-22.992		
$7P_{1/2}$	0.015				0.064	-0.064		
$8P_{1/2}$	0.014				0.011	-0.011		
$6P_{3/2}$	74.560				3.846	3.077	24.210	-24.210
$7P_{3/2}$	0.043				0.021	0.017	0.116	-0.116
$8P_{3/2}$	0.014				0.003	0.003	0.019	-0.019
$5D_{3/2}$		-45.984	-3.846	-3.077				
$6D_{3/2}$		68.101	8.275	6.620				
$7D_{3/2}$		4.163	0.434	0.347				
$5D_{5/2}$			-36.315	7.263				
$6D_{5/2}$			72.167	-14.433				
$7D_{5/2}$			3.895	-0.779				
$4F_{5/2}$					11.857	-2.371	0.668	0.763
$5F_{5/2}$					1.643	-0.329	0.089	0.102
$6F_{5/2}$					0.017	-0.003	0.009	0.010
$4F_{7/2}$							13.344	-4.766
$5F_{7/2}$							2.655	-0.948
$6F_{7/2}$							0.430	-0.154
Others	9.137	11.304	11.716	-0.508	8.981	-0.019	9.000	-0.084
Total	124.546(1.256)	17.379(2.920)	45.890(3.831)	5.870(128)	49.435(1.458)	-22.694(538)	50.540(1.410)	-29.422(931)
Expt. [34]	123.88(5)							
[35]	125.5(10)							
Theory [16]	124.15							
[36]	123.07							
[37]	126.2							
[38]	124.7							

TABLE VI: Absolute magnitudes of the reduced dipole matrix elements in Ra^+ . Estimated error bars from this work given inside the parenthesis.

Transition	Present	Ref. [14]	Ref. [18]
$7p_{1/2} \rightarrow 7s_{1/2}$	3.28(2)	3.224	3.2545
$8p_{1/2} \rightarrow 7s_{1/2}$	0.08(4)	0.088	
$9p_{1/2} \rightarrow 7s_{1/2}$	0.09(3)	0.116	
$7p_{3/2} \rightarrow 7s_{1/2}$	4.54(2)	4.477	4.5106
$8p_{3/2} \rightarrow 7s_{1/2}$	0.49(2)	0.339	
$9p_{3/2} \rightarrow 7s_{1/2}$	0.30(2)	0.095	
$7p_{1/2} \rightarrow 6d_{3/2}$	3.62(5)	3.550	3.5659
$8p_{1/2} \rightarrow 6d_{3/2}$	0.06(2)	0.013	
$9p_{1/2} \rightarrow 6d_{3/2}$	0.02(1)	0.013	
$7p_{3/2} \rightarrow 6d_{3/2}$	1.54(2)	1.504	1.5117
$8p_{3/2} \rightarrow 6d_{3/2}$	0.15(2)	0.127	
$9p_{3/2} \rightarrow 6d_{3/2}$	0.07(2)	0.057	
$5f_{5/2} \rightarrow 6d_{3/2}$	4.67(2)		4.4491
$6f_{5/2} \rightarrow 6d_{3/2}$	0.86(4)		
$7f_{5/2} \rightarrow 6d_{3/2}$	0.48(11)		
$7p_{3/2} \rightarrow 6d_{5/2}$	4.83(8)	4.816	4.8232

TABLE VII: Dynamic vector polarizabilities (in au) at two different wavelengths in Ra^+ .

Intermediate States (K)	$7s_{1/2}$		$6d_{3/2}$	
	$\lambda = 514.53\text{nm}$	$\lambda = 1111.68\text{nm}$	$\lambda = 514.53\text{nm}$	$\lambda = 1111.68\text{nm}$
$7p_{1/2}$	-391.483	-37.764	31.921	-869.894
$8p_{1/2}$	-0.008	-0.003	-0.002	-8×10^{-4}
$9p_{1/2}$	-0.007	-0.003	-1×10^{-4}	-5×10^{-5}
$7p_{3/2}$	94.788	22.384	3.784	-2.632
$8p_{3/2}$	0.144	0.059	-0.005	-0.002
$9p_{3/2}$	0.035	0.015	-6×10^{-4}	-3×10^{-4}
$5f_{5/2}$			9.452	3.361
$6f_{5/2}$			0.149	0.061
$7f_{5/2}$			0.035	0.015
Others	0.323	0.145	0.795	0.345
Total	-296.207(4.909)	-15.167(255)	46.128(679)	-868.749(24.027)

TABLE VIII: Transition strengths (au), wavelengths (\AA) and probabilities ($\times 10^6 s^{-1}$) from P-states in Ra^+ .

Transition($f \rightarrow i$)	$S_{f \rightarrow i}^{E1}$	$\lambda_{f \rightarrow i}$	$A_{f \rightarrow i}^{E1}$
$A_{7P_{1/2} \rightarrow 7S_{1/2}}$	11.086	4683.6	106.083
$A_{7P_{3/2} \rightarrow 7S_{1/2}}$	20.612	3815.5	187.960
$A_{7P_{1/2} \rightarrow 6D_{3/2}}$	13.104	10791.2	10.564
$A_{7P_{3/2} \rightarrow 6D_{3/2}}$	2.372	7080.0	3.385
$A_{7P_{3/2} \rightarrow 6D_{5/2}}$	23.329	8022.0	22.890

TABLE IX: Net transition probabilities ($\times 10^6 s^{-1}$) and lifetimes (ns) in Ra^+ .

State(= i)	A_i	τ_i
$7P_{1/2}$	116.647	8.57(12)
$7P_{3/2}$	214.235	4.67(5)